18. J. Jonsson, L. Carlsson, T. Edlund, H. Edlund, *Nature* **371**, 606 (1994).
19. M. F. Offield *et al.*, *Development* **122**, 983 (1996).
20. J. Nichols *et al.*, *Cell* **95**, 379 (1998).
21. M. Schuldiner, O. Yanuka, J. Itskovitz-Eldor, D. A. Melton, N. Benvenisty, *Proc. Natl. Acad. Sci. U.S.A.* **97**, 11307 (2000).
22. K. Gerrish *et al.*, *J. Biol. Chem.* **275**, 3485 (2000).
23. D. A. Stoffers, R. S. Heller, C. P. Miller, J. F. Habener, *Endocrinology* **140**, 5374 (1999).
24. Cells were fixed in 4% paraformaldehyde/0.15% picric acid in phosphate-buffered saline (PBS). Immunocytochemistry was carried out with the use of standard protocols. The following primary antibodies were used at following dilutions: nestin rabbit polyclonal 1:500 (made in our laboratory), TUJ1 mouse monoclonal 1:500 and TUJ1 rabbit polyclonal 1:2000 (both from Babco, Richmond, CA), insulin mouse monoclonal 1:1000 (Sigma, St. Louis, MO), insulin guinea pig polyclonal 1:100 (DAKO, Carpinteria, CA), glucagon rabbit polyclonal 1:75 (DAKO), somatostatin rabbit polyclonal 1:100 (DiaSorin, Stillwater, MN), GFP 1:750 polyclonal (Molecular Probes, Eugene, OR), and BRDU rat monoclonal 1:100 (Accurate, antibodies, Westbury, NY). For detection of primary antibodies, fluorescently labeled secondary antibodies (Jackson Immunoresearch Laboratories, West Grove, PA, and Molecular Probes) were used according to methods recommended by the manufacturers. Histochemical staining for alkaline phosphatase cells was carried out using commercially available kit (Sigma) following manufacturer's recommendations.
25. A. Ferreira, A. Caceres, *J. Neurosci. Res.* **32**, 516 (1992).
26. W. W. Kao *et al.*, *Ophthalmol. Vis. Sci.* **37**, 2572 (1996).
27. K. Hadjantonakis, M. Gertsenstein, M. Ikawa, M. Okabe, A. Nagy, *Mech. Dev.* **76**, 79 (1998).
28. For counting of insulin-positive cells, stage 5 ES cell cultures 6 days after bFGF withdrawal were dislodged from tissue culture surface in Ca^{2+}-free 3 mM EDTA containing Krebs-Ringer buffer after incubation for 15 min at 37°C. The clusters were dissociated into single cells, as previously described (*29*). Dissociated cells were allowed to adhere to poly-ornithine/laminine-coated glass coverslips for 5 hours, fixed, immunostained for insulin, and counterstained with a nuclear stain DAPI (4′,6′diamidino-2-phenylindole). This was followed by determination of the percentage of insulin-positive cells in the total cell population.
29. C. B. Wollheim, P. Meda, P. A. Halban, *Methods Enzymol.* **192**, 188 (1990).
30. Stage 3 GFP-labeled B5 ES cells were co-cultured at clonal density on poly-ornithine/fibronectin treated–96-well plates [Costar 3603 (Fisher Scientific, Pittsburgh, PA) black plate with clear and thin bottom] with stage 3 wild-type E14.5 ES cells at a final concentration of 1 B5 cell per 40,000 E14.5 cells per well. B5 cells were plated at a concentration of 1 B5 cell per well using serial dilution. The seeding efficiency and the growth of the plated B5 cells were monitored by immunocytochemical staining for GFP. Two hours after seeding, GFP-positive cells were present in 65 ± 5% of the wells. Counterstaining with a nuclear dye (DAPI) confirmed presence of only one cell per well. After 6 days of differentiation, single GFP-labeled clones derived from a single B5 cell were present in 14.8 ± 1.7% of the wells. Cells were cultured through stages 4 and 5, as shown in Fig. 1A. On day 6 of stage 5, cells were fixed with 4% paraformaldehyde and subjected to triple immunocytochemistry and laser confocal microscopy analysis. For immunocytochemistry, after blocking with a solution of 90% PBS, 10% normal goat serum, and 0.3% Triton-X100, cells were stained with antibodies against insulin [mouse immunoglobulin G1 (IgG1)], GFP (mouse IgG2a), and TUJ1 (rabbit). Cy5, FITC, and Cy3-conjugated goat antibodies to IgG1 mouse, IgG2a mouse and IgG rabbit, respectively, were used as secondary antibodies.
31. S. H. Orkin, *Nature Med.* **6**, 1212 (2000).
32. The cells were labeled with BrdU (Boehringer Mannheim, Indianapolis, IN) at final concentration 10 μm for 24 hours. After the labeling, depending on the specific experiment, the cells were either fixed immediately in 4% paraformaldehyde/0.15% picric acid, treated with 95% ethanol/5% glacial acidic acid for 15 min at room temperature, and subjected to immunocytochemistry, or they were cultured for various lengths of time and then analyzed by immunocytochemistry.
33. A. Vinik, R. Rafaeloff, G. Pittenger, L. Rosenberg, W. Duguid, *Horm. Metab. Res.* **29**, 278 (1997).
34. Insulin secretion was measured using static incubations in Krebs-Ringer with bicarbonate buffer as follows: 120 mM NaCl, 5 mM KCl, 2.5 mM $CaCl_2$, 1.1 mM $MgCl_2$, 25 mM $NaHCO_3$, and 0.1% bovine serum albumin at 37°C. Inhibitors of insulin secretion (nifedipine and diazoxide) were added to the incubation buffer 30 min before addition of glucose. For determination of total cellular insulin content, insulin was extracted from cells with acid ethanol (10% glacial acetic acid in absolute ethanol) overnight at 4°C, followed by cell sonication. Total cellular and secreted insulin was assayed using insulin enzyme-linked immunosorbence assay (ELISA) kit (ALPCO, Windham, NH). Protein concentrations were determined using DC protein assay system (Bio-Rad, Hercules, CA).
35. V. J. Csernus, T. Hammer, D. Peschke, E. Peschke, *Cell. Mol. Life Sci.* **54**, 733 (1998).
36. N. H. McClenaghan, P. R. Flatt, *J. Mol. Med.* **77**, 235 (1999).
37. G. Trube, P. Rorsman, T. Ohno-Shosaku, *Pflugers Arch.* **407**, 493 (1986).
38. W. Montague, J. R. Cook, *Biochem. J.* **122**, 115 (1971).
39. B. Ahren, S. Karlsson, S. Lindskog, *Prog. Brain Res.* **84**, 209 (1990).
40. E. Rojas, J. Hidalgo, P. B. Carroll, M. X. Li, I. Atwater, *FEBS Lett.* **26**, 265 (1990).
41. All animal studies were in accordance with NIH institutional guidelines. Experimental diabetes was induced in 10- to 12-week-old male 129/sv mice (Taconic, Germantown, NY) by a single intraperitoneal injection (150 mg/kg of body weight) of streptozotocin (Sigma) freshly dissolved in 0.1 M of citrate buffer, pH 4.5. Stable hyperglycemia (blood glucose levels 300 to 600 mg/dl) usually developed 48 to 72 hours after the streptozotocin injections. Blood glucose level was determined using Glucometer Elite XL blood glucose meter (Bayer Corp., Elkhart, IN). The animals were grafted with cells or with a buffer vehicle 24 to 48 hours after the establishment of stable hyperglycemia. Injected into each animal were 1 to 2 × 10^7 cells in the form of cluster suspension. In most experiments, day 6 stage 5 cells were used, suspended in Krebs-Ringer–bicarbonate buffer without Ca^{2+}, and injected subcutaneously under isofluorine anesthesia in the shoulder area through a 19-gauge hypodermic needle. To prepare the cluster suspension, the cells cultured on 60-mm tissue culture dishes were carefully dislodged by treatment with Krebs-Ringer–bicarbonate buffer without Ca^{2+} and with 3 mM EDTA for 5 min at 37°C. Each experimental group consisted of five to eight animals per group. The animals were killed at different times, and the grafts were excised and fixed in 4% paraformaldehyde/0.15% picric acid in PBS. Sections of the grafts (15 to 20 μm) were analyzed by immunohistochemistry.
42. P. A. Halban, S. L. Powers, K. L. George, S. Bonner-Weir, *Diabetes* **36**, 783 (1987).
43. B. Soria *et al.*, *Diabetes* **49**, 157 (2000).
44. B. E. Reubinoff, M. F. Pera, C. Y. Fong, A. Trounson, A. Bongso, *Nature Biotechnol.* **18**, 399 (2000).
45. V. K. Ramiya *et al.*, *Nature Med.* **6**, 278 (2000).
46. S. Bonner-Weir *et al.*, *Proc. Natl. Acad. Sci. U.S.A.* **97**, 7999 (2000).
47. A. M. Shapiro *et al.*, *N. Engl. J. Med.* **27**, 230 (2000).
48. We thank T. Doetschman for gift of E14.1 ES cells and A. Nagy for gift of B5 ES cells. We also thank C. Smith for her help with confocal microscopy and J.-H. Kim for alkaline phosphatase analysis of ES cells. I.V. was supported by a fellowship from the PEW charitable Trust. We thank the National Parkinsons Foundation for their support of our work and C. Gerfen for many positive contributions.

8 January 2001; accepted 13 April 2001
Published online 26 April 2001;
10.1126/science.1058866
Include this information when citing this paper.

Autosomal Recessive Hypercholesterolemia Caused by Mutations in a Putative LDL Receptor Adaptor Protein

Christine Kim Garcia,[1] Kenneth Wilund,[1,2] Marcello Arca,[3] Giovanni Zuliani,[4] Renato Fellin,[4] Mario Maioli,[5] Sebastiano Calandra,[6] Stefano Bertolini,[7] Fausto Cossu,[8] Nick Grishin,[9] Robert Barnes,[1] Jonathan C. Cohen,[1] Helen H. Hobbs[1,2*]

Atherogenic low density lipoproteins are cleared from the circulation by hepatic low density lipoprotein receptors (LDLR). Two inherited forms of hypercholesterolemia result from loss of LDLR activity: autosomal dominant familial hypercholesterolemia (FH), caused by mutations in the *LDLR* gene, and autosomal recessive hypercholesterolemia (ARH), of unknown etiology. Here we map the *ARH* locus to a ~1-centimorgan interval on chromosome 1p35 and identify six mutations in a gene encoding a putative adaptor protein (ARH). ARH contains a phosphotyrosine binding (PTB) domain, which in other proteins binds NPXY motifs in the cytoplasmic tails of cell-surface receptors, including the LDLR. ARH appears to have a tissue-specific role in LDLR function, as it is required in liver but not in fibroblasts.

The liver is the major site of synthesis and clearance of cholesteryl ester–rich lipoproteins. More than 70% of circulating LDL is removed from the blood via hepatic LDLR-mediated endocytosis (*1*). In individuals with two mutant LDLR alleles (homozygous FH), the rate of clearance of LDL from the blood is decreased, resulting in hypercholesterolemia, xanthomatosis (deposition of cholesterol in skin and tendons) and premature coronary artery disease (CAD) (*1*). LDLR activity in cultured skin fibroblasts from FH homozygotes is also very low (*1*). A rare autosomal recessive form of hypercholesterolemia (ARH) that clinically resembles FH but is not due to mutations in *LDLR* has been described (*2–9*). These patients have markedly impaired hepatic LDLR function but normal or only modestly reduced LDLR function in cultured fibroblasts (*3–5, 7, 8*).

To elucidate the molecular basis of ARH we performed a whole-genome linkage study in four ARH families (Fig. 1A). Two were of Sardinian origin and had low LDL clearance rates in vivo (ARH1 and ARH2) (*8*), and two were of Lebanese origin (ARH3 and ARH4), including the original family described with this disorder (*2*). The probands of the four families were offspring of consanguineous unions and all families showed horizontal transmission of hypercholesterolemia. All affected family members were severely hypercholesterolemic and had very large xanthomas; some had premature CAD (Table 1). Plasma LDL levels tended to be lower and the onset of symptomatic CAD somewhat later in these probands than in FH homozygotes. LDLR function in cultured fibroblasts from affected family members were normal or only moderately reduced (*3, 7, 8*), thus ruling out a diagnosis of homozygous FH.

Multipoint linkage analysis revealed significant linkage [logarithm of the odds ratio for linkage (lod) score, 7.4] to a 5.7-cM interval on 1p35, demarcated by the polymorphic loci D1S2864 and D1S2787 (Fig. 1B) (*10*). This interval overlaps to a chromosomal region on 1p35–p36 linked to ARH in two other families (*11*). We found no linkage to 15q25–q26, which was previously found to be associated with ARH in five Sardinian

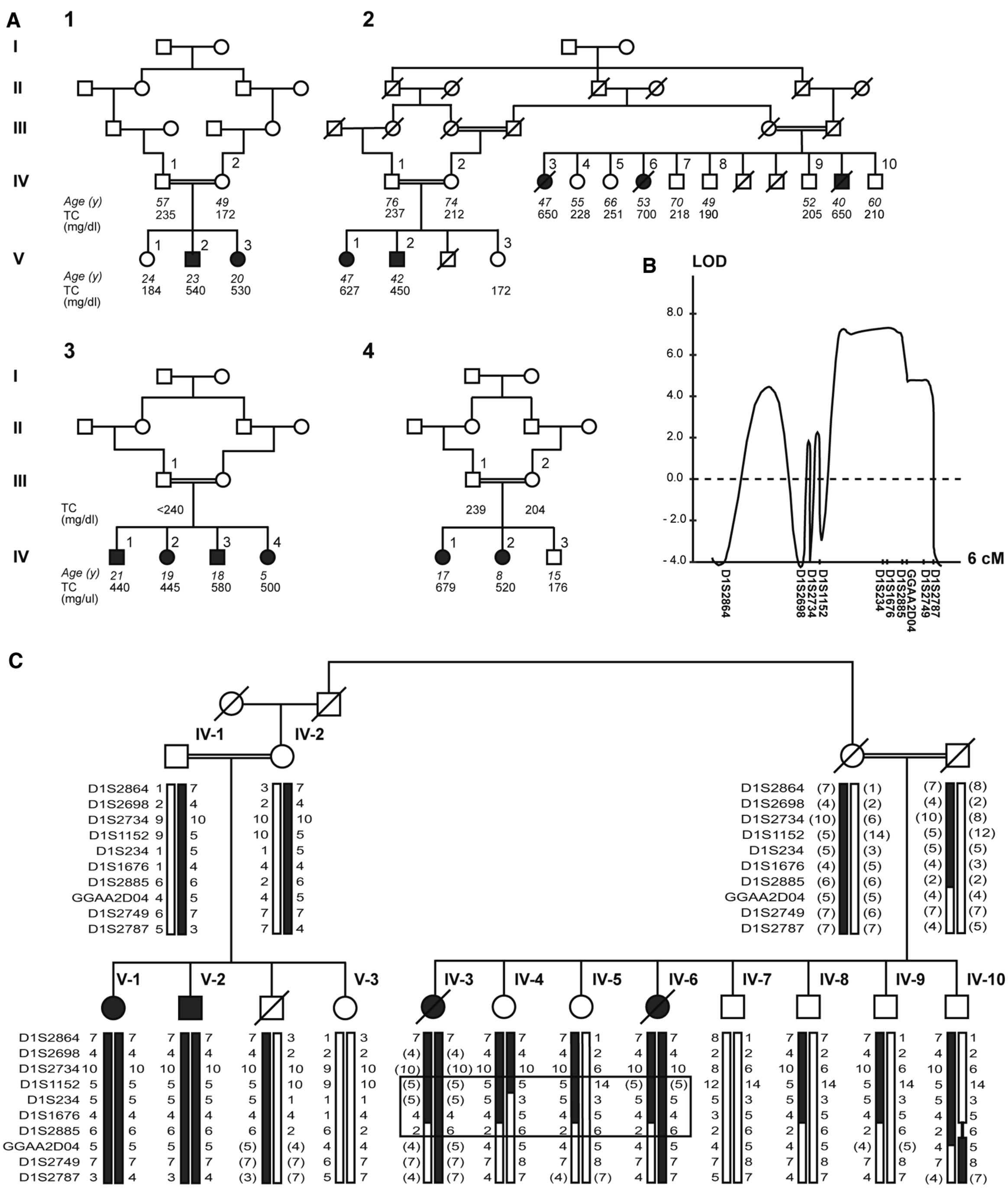

Fig. 1. Pedigrees (A), linkage analysis (B), and fine mapping (C) of the *ARH* gene. (**A**) The four pedigrees used for gene mapping (ARH1 to ARH4) are shown. ARH1 and ARH2 are Sardinians, and ARH3 and ARH4 are Lebanese. Fasting plasma total cholesterol levels (TC) are shown. (**B**) Distribution of lod scores in the linked region on chromosome 1. A total genome scan was performed initially in ARH1 and ARH2 and then additional markers were typed in all four families. The maximum lod score was 7.4 over a ~1-cM region on chromosome 1. (**C**) Fine mapping within the linked region in ARH2. Genomic DNA was extracted from whole blood that had been collected from the deceased probands and stored at –20°C for more than 10 years, or from fresh leukocytes isolated from venous blood. The region of homozygosity shared by the affected individuals in this family is boxed. Squares, males; circles, females; double lines, consanguineous matings; filled squares, affected individuals.

families (*9*), including ARH1 (Fig. 1). We refined the linked region to a ~1-cM interval extending from D1S1152 to D1S2885 by identifying a region of homozygosity shared by all affected family members but not by a normocholesterolemic sibling in ARH2 (Fig. 1C) (*12*). The coding sequences of 13 genes that mapped to this interval were screened for sequence variation by PCR and the single strand conformation polymorphism (SSCP) technique (*13*). Two abnormally migrating bands were identified in the predicted coding sequences of a cDNA (DKFZp586D0624) in probands from ARH1 and ARH3.

The gene structure and predicted amino acid sequence of the protein encoded by this cDNA are shown in Fig. 2. The gene spans ~25 kb and has nine exons and eight introns (Fig. 2A). The predicted amino acid sequence contains a 170–amino acid motif that shares considerable sequence similarity with the phosphotyrosine binding (PTB) domains of many adaptor proteins (*14, 15*) (Fig. 2B). PTB domains bind the consensus sequence NPXY, which is present in the cytoplasmic domains of several cell-surface receptors, including the epidermal growth factor receptor (*16*), the insulin receptor (*17*), nerve growth factor receptor (TrkA) (*18*), and the LDLR (*19, 20*). The integrity of the NPXY sequence in the cytoplasmic tail of the LDLR is absolutely required for internalization (*19, 20*), and the LDLR has been shown in vitro to bind other proteins containing PTB domains (*21, 22*).

[1]McDermott Center for Human Growth and Development and Department of Internal Medicine and [2]Molecular Genetics, [9]Howard Hughes Medical Institute and Department of Biochemistry, University of Texas Southwestern Medical Center at Dallas, 5323 Harry Hines Boulevard, Dallas, TX 75390, USA. [3]Institute of Systematic Medical Therapy, University of Rome "La Sapienza," Rome 00161, Italy. [4]Department of Internal Medicine, University of Ferrara, Ferrara 44100, Italy. [5]Metabolic Disease Unit, Department of Internal Medicine, University of Sassari, Sassari 07100, Italy. [6]Department of Biological Science, University of Modena and Reggioemilia, Modena 41100, Italy. [7]Department of Internal Medicine, University of Genoa, Genoa 16100, Italy. [8]Bone Marrow Transplant Unit, Ospedale Microcitemico, Cagliari 09121, Italy.

*To whom correspondence should be addressed. Email: helen.hobbs@UTSouthwestern.edu

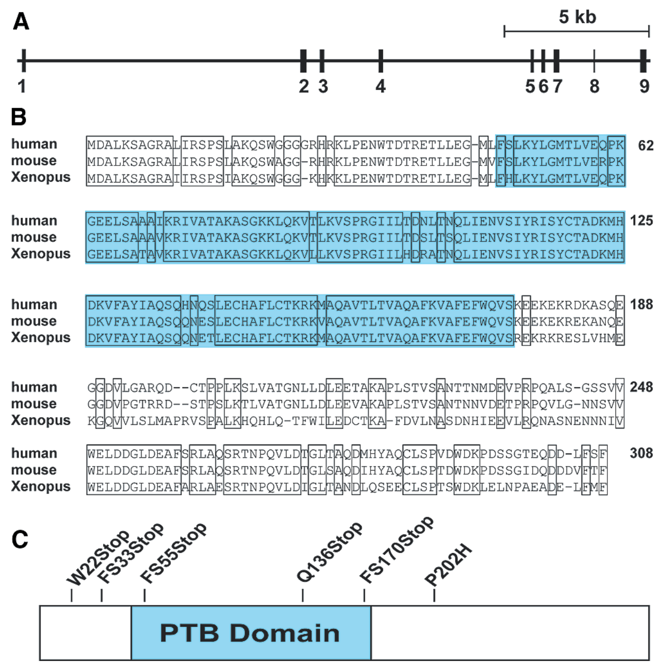

Fig. 2. Gene structure (A), predicted amino acid sequence (B), and location of mutations in ARH probands (C). (**A**) The cDNA for DKFZp586D0624 (GenBank Accession Number AL117654) was prepared by PCR amplification of reverse-transcribed liver poly(A)$^+$ mRNA. A P_1 clone containing the entire gene (290N7, Incyte Genomics, Inc., Palo Alto) was used to amplify the introns and to sequence intron-exon boundaries. *ARH* is encoded by nine exons and spans ~25 kb. Filled rectangles, exons; lines, introns. (**B**) The predicted amino acid sequences of human, mouse, and *Xenopus* ARH. Numbers to the right correspond to human sequence. The alignment of the inferred amino acid sequences displays 67% identity among the three proteins. The regions of amino acid identity are boxed. ARH has a highly conserved PTB domain at the amino terminus (indicated by blue shading, 89% identity). Alignment was constructed with PSI-BLAST (*23*). The boundaries of the PTB domain are according to Pfam 6.0 database [(*35, 36*); domain PF00640]. (**C**) Schematic representation of ARH showing the location of the mutations identified in this study.

Table 1. Molecular defects in ARH and clinical characteristics of probands in four families with ARH (Fig. 1). Genomic DNA was extracted from cultured fibroblasts or leukocytes. The coding regions of the gene were screened for sequence variation using SSCP and dideoxy sequencing. The nucleotides and amino acids were numbered from the A of the initiation codon (ATG). The age at the time of diagnosis is provided. The plasma cholesterol and LDL-cholesterol levels were measured by the referring physician. LDLR activity was assessed as described in the reference and is provided as a percentage of normal control fibroblasts studied simultaneously. Abbreviations: TC, fasting plasma total cholesterol; ref., reference; ins, insertion; F, female; CAD, symptomatic or documented coronary artery disease; AS, aortic murmur or stenosis; yr, years; M, male; ND, not done; NIDDM, non–insulin-dependent diabetes; Tx, treatment; MI, myocardial infarction; del, deletion; X, stop; amino acids: W, tryptophan; Q, glutamine; P, proline; H, histidine.

Family	Nucleotide change	Amino acid change	Origin	Age/ sex	Plasma TC/ LDL-C (mg/dl)	LDLR activity in fibroblasts (%)	Comments	Ref.
ARH1	c.432insA	170Stop	Nuoro, Sardinia	20/F	530/460	~70	CAD, AS; eight relatives died at <33 years	(*3, 7–9*)
				23/M	540/464	~80	CAD, AS	
ARH2	c.65G>A	W22X	Olbia, Sardinia	40/M	650/ND	ND	CAD	(*8*)
				53/F	700/ND	ND	CAD, NIDDM	
				47/F	650/ND	ND	CAD, TC = 369 on Tx	
				47/F	627/550	80	CAD	
				42/M	450/372	85		
ARH3	c.406C>T	Q136X	Beirut, Lebanon	21/M	440/ND	60–70	Father, NIDDM	(*2, 3*)
				19/F	445/ND			
				18/M	580/ND	60–70		
				5/F	500/ND			
ARH4	c.605C>A	P202H	Lebanon	17/F	610/520	100	Father, MI, 28 years	(*3*)
				7/F	520/392	100		
ARH5	c.72insG	33Stop	Iran	10/M	637/598	ND		
ARH6	c.71delG	55Stop	USA	15/F	800	ND	AS, TC = 321 on Tx	

Database searches (*23*) revealed orthologous proteins in mouse and *Xenopus* that share 89% sequence identity with the human protein in the PTB domain (Fig. 2B). Several regions in the COOH-terminal half of these protein are also highly conserved. These blocks do not appear to be shared with other proteins currently in the database. The closest paralogs of ARH are the *Drosophila* NUMB protein (*24*) and the *Caenorhabditis elegans* CED-6, an adaptor protein involved in cell engulfment (*25*). These proteins share 33% (52%) and 34% (60%) sequence identity (similarity) with the human protein, respectively.

The coding region of ARH was sequenced using genomic DNA from the affected family members of ARH1, ARH2, ARH3, and ARH4 (Fig. 1). Two different mutations that cause premature termination of translation were identified in the Sardinian families. The affected individuals in ARH1 were homozygous for a single base-pair insertion in exon 4 (Table 1) that introduces a premature termination codon at amino acid 170, truncating the protein in the terminal portion of the PTB domain. Affected individuals in ARH2 were homozygous for a nonsense mutation at codon 22. The ARH gene was sequenced in 10 other unrelated Sardinian probands. Four Sardinian patients were homozygous for the frameshift mutation in exon 4, and three were homozygous for the nonsense mutation in exon 1. The remaining three probands were compound heterozygotes for the two mutations. The finding that only two mutations account for ARH in these 12 apparently unrelated Sardinian probands probably reflects genetic drift, which has been observed for other diseases on the island (*26, 27*). There was significant overlap in the distribution of the mutation on the island; neither mutation was found in 50 normolipidemic Sardinians (*28*).

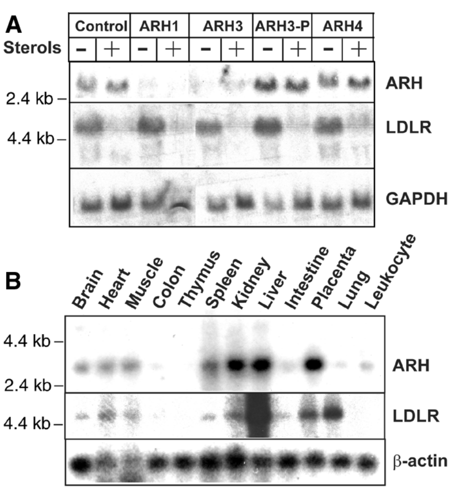

Fig. 3. Expression of ARH and LDLR in fibroblasts (A) and human tissues (B). (**A**) Fibroblasts were plated at a density of 1.5 × 10^5 in 100-mm dishes and grown in 5% fetal calf serum (FCS). On day 4, the medium was changed to 10% human lipoprotein–poor serum (HLPPS) (minus sterols) or 10% FCS (plus sterols). Cells were harvested on day 5, and total RNA was isolated using RNA-STAT-60 (Tel-Test, Inc., Friendswood, Texas). Northern blotting was performed using 20 μg of RNA (*37*). The coding regions of ARH, LDLR, and GAPDH (as a loading control) were amplified by PCR, and the fragments were radiolabeled (Megaprime DNA Labeling System, Amersham Pharmacia Biotech, Piscataway, New Jersey) before incubation with the filter (1 × 10^6 cpm/ml). ARH3-P, father of proband for ARH-3. (**B**) Northern blot analysis of human tissues. Radiolabeled ARH, LDLR, and β-actin probes were incubated with the RNA blot (Clontech Laboratories, Inc., Palo Alto, California) in Rapid-Hyb buffer (Amersham) (1 × 10^6 cpm/ml).

The four affected Lebanese siblings in ARH3 (Fig. 1) were homozygous for a nonsense mutation in codon 136, which stops translation in the terminal region of the PTB binding domain. Both ARH4 probands were homozygous for a missense mutation substituting a histidine for proline at amino acid 202, which is outside the PTB domain. The LDLR activity was normal in the ARH3 fibroblasts (*3*). Neither of the mutations found in ARH3 or ARH4 was present in 15 normolipidemic individuals from Lebanon, seven unrelated Lebanese FH homozygotes with a molecularly defined defect in the LDLR gene (*29*), or in 50 normocholesterolemic Caucasians. ARH probands from two other unrelated consanguineous families (ARH5 and ARH6) were homozygous for different frameshift mutations located in a string of seven guanine residues in exon 1 (Table 1). Both mutations are predicted to truncate the protein near the NH_2-terminus (Fig. 2C).

We performed Northern blot analysis to assess the size and relative abundance of the ARH mRNA in cultured fibroblasts from the probands of the ARH1, ARH3, and ARH4 families (Fig. 3A). A 3.1-kb mRNA was detected in the control fibroblasts. In contrast to the LDLR mRNA, the levels of ARH mRNA were not affected by the addition of sterols to the medium. Only trace amounts of ARH mRNA were detected in the ARH1 fibroblasts, in which both ARH alleles contained the frameshift mutation in exon 4, and in the ARH3 fibroblasts, in which were homozygous for a nonsense mutation in exon 4. Normal levels of ARH mRNA were present in the ARH4 fibroblasts, which harbored a homozygous missense mutation. Studies are in progress to determine the functional effects of this mutation. ARH4 was the only family in which the parents had evidence of a possible defect in cholesterol metabolism; the father had a myocardial infarction at age 28. In one ARH family described by Norman *et al*. (6), both parents had moderately elevated plasma LDL-cholesterol levels. These observations raise the possibility that some ARH mutations result in codominant, rather than recessive hypercholesterolemia.

Preliminary results using a mammalian two-hybrid system indicate that the PTB domain of ARH interacts with the cytoplasmic tail of the LDLR, and additional studies are under way to characterize the specificity and physiological significance of this interaction. PTB domains differ in their selectivity for NPXY sequences in different proteins, which allows for specificity in the biological response (*30*). For example, the *Drosophila* SHC (*30*) and mouse Disabled (*21*) adaptor proteins, bind to only a subset of NPXY sequences. ARH appears to be a close phenocopy of homozygous FH, which suggests that all clinical sequelae of ARH mutations are attributable to defective LDLR activity, and this in turn suggests that ARH binds specifically to the LDLR. However, although both ARH and LDLR appear to be nearly ubiquitously expressed (Fig. 3B), LDLR expression is relatively low in some of the same tissues that express high levels of ARH (kidney, placenta) (*1*), raising the possibility that this protein may be involved in other receptor pathways. None of the 16 probands examined in this study have other obvious shared phenotypes that would suggest defective signaling or functioning of NPXY-containing proteins, with the possible exception of NIDDM (non–insulin-dependent diabetes mellitus) (Table 1).

The defect in LDLR function in ARH appears to be not only receptor-specific, but also tissue-specific. We have been unable to identify a consistent defect in LDLR function (binding, uptake or internalization) in cultured fibroblasts from ARH patients. It is possible that another PTB domain protein compensates for the absence of ARH in cultured fibroblasts, or that adaptor molecules are not required for receptor-medicated endocytosis of LDL in fibroblasts and possibly other extrahepatic cells.

ARH may participate in a step in the itinerary of the LDLR pathway that is specific to polarized cells like hepatocytes (*31*). ARH may be required for trafficking of LDLR to the basolateral surface. In contrast to fibroblasts, LDLRs in hepatocytes do not cluster in coated pits; conceivably, ARH may target the LDLR to the coated pit after the receptor binds LDL (*32*). Alternatively, ARH may participate in the recycling of the LDLR from the lysosome to the basolateral cell surface after dissociating from LDL. Although the specific role of ARH in the functioning of the LDLR remains to be defined, the crucial role of this protein is revealed by the profound hypercholesterolemia that occurs in this disease.

References and Notes

1. J. L. Goldstein, H. H. Hobbs, M. S. Brown, in *The Metabolic and Molecular Bases of Inherited Disease*, C. R. Scriver *et al.*, Eds. (McGraw-Hill, New York, ed. 8, 2001), vol. II, chap. 120, pp. 2863–2913.
2. A. K. Khachadurian, S. M. Uthman, *Nutr. Metab*. **15**, 132 (1973).
3. J. L. Goldstein, M. S. Brown, unpublished observations.

4. M. Harada-Shiba *et al.*, *Arterioscler. Thromb.* **12**, 1071 (1992).
5. H. H. Schmidt *et al.*, *J. Clin. Endocrinol. Metab.* **83**, 2167 (1998).
6. D. Norman *et al.*, *J. Clin. Invest.* **104**, 619 (1999).
7. G. Zuliani *et al.*, *Eur. J. Clin. Invest.* **25**, 322 (1995).
8. G. Zuliani *et al.*, *Arterioscler. Thromb. Vasc. Biol.* **19**, 802 (1999).
9. M. Ciccarese *et al.*, *Am. J. Hum. Genet.* **66**, 453 (2000).
10. A whole-genome linkage analysis was performed using 450 polymorphic DNA markers at ~8-cM intervals (Cooperative Human Linkage Center/Weber Human Screening Set Version 8, Research Genetics, Inc., Huntsville). Markers were genotyped in selected family members from ARH1 (IV.1, IV.2, V.1, V.2, V.3) and ARH2 (IV.1, IV.2, V.1, V.2, V.3) (Fig. 1). Linkage analysis using GENEHUNTER (*33*) and CRIMAP (*34*), ruled out linkage to 93% of the genome. An additional 70 genetic markers covering the 14 genomic regions that could not be excluded on the initial genome-wide screen were genotyped in all numbered members of the four families (Fig. 1A). Linkage to a region on 1p35 was found with a lod score of 7.4. The affected siblings in ARH1 and ARH3 had inherited alleles identical by descent in this region but were not homozygous for any of the markers. The two siblings of ARH4 shared a 44-cM region of homozygosity in this region.
11. E. Eden, R. Naoumova, J. Burden, M. McCarthy, A. Soutar, *Am. J. Hum. Genet.* **68**, 653 (2001).
12. The centrometric boundary of homozygosity was defined by D1S2885 (family members IV.3 and IV.6 in ARH2), which is telomeric to GGAA2D04 on the physical map (www.ncbi.nlm.nih.gov). The telomeric boundary was delineated by marker D1S1152 in individual IV.4, who was normolipemic and yet was homozygous for the markers distal to D1S1152. The exact position of D1S1152 was determined through genetic analysis of crossovers in ARH2 and CEPH family no. 1362. The coding regions of the genes located in the physical region between markers D1S1152 and D1S2885 were screened for sequence variations.
13. M. Orita, Y. Suzuki, T. Sekiya, K. Hayashi, *Genomics* **5**, 874 (1989).
14. M. M. Zhou, S. W. Fesik, *Prog. Biophys. Mol. Biol.* **64**, 221(1995).
15. P. Bork, B. Margolis, *Cell* **80**, 693 (1995).
16. P. Blaikie *et al.*, *J. Biol. Chem.* **269**, 32031(1994).
17. W. He, T. J. O'Neill, T. A. Gustafson, *J. Biol. Chem.* **270**, 23258 (1995).
18. A. Obermeier *et al.*, *EMBO J.* **13**, 1585 (1994).
19. C. G. Davis *et al.*, *Cell* **45**, 15 (1986).
20. W.-J. Chen, J. L. Goldstein, M. S. Brown, *J. Biol. Chem.* **265**, 3116 (1990).
21. M. Trommsdorff, J. P. Borg, B. Margolis, J. Herz, *J. Biol. Chem.* **273**, 33556 (1998).
22. M. Gotthardt *et al.*, *J. Biol. Chem.* **275**, 25616 (2000).
23. S. F. Altschul *et al.*, *Nucleic Acids Res.* **25**, 3389 (1997)
24. J. A. Knoblich, L. Y. Jan, Y. N. Jan, *Proc. Natl. Acad. Sci. U.S.A.* **94**, 13005 (1997).
25. Q. A. Liu, M. O. Hengartner, *Cell* **93**, 961 (1998).
26. M. C. Rosatelli *et al.*, *Am. J. Hum. Genet.* **50**, 422 (1992).
27. G. Loudianos *et al.*, *Hum. Mutat.* **14**, 294 (1999).
28. M. Arca, G. Zuliani, unpublished data
29. M. A. Lehrman *et al.*, *J. Biol. Chem.* **262**, 401 (1987).
30. S. Luschnig, J. Krauss, K. Bohmann, I. Desjeux, C. Nusslein-Volhard, *Mol. Cell* **5**, 231 (2000).
31. K. Matter, J. A. Whitney, E. M. Yamamoto, I. Mellman, *Cell* **74**, 1053 (1993).
32. R. K. Pathak *et al.*, *J. Cell Biol.* **111**, 347 (1990).
33. L. Kruglyak, M. J. Daly, M. P. Reeve-Daly, E. S. Lander, *Am. J. Hum. Genet.* **58**, 1347 (1996).
34. E. S. Lander, D. Botstein, *Science* **236**, 1567 (1987).
35. A. Bateman *et al.*, *Nucleic Acids Res.* **28**:263 (2000).
36. http://pfam.wustl.edu
37. E. V. Jokinen *et al.*, *J. Biol. Chem.* **269**, 26411 (1994).

38. We thank E. Kern, Y. Liao, R. Wilson, J. Hunter, and B. Crider and especially T. Hyatt for excellent technical assistance; A. Cao, A. Montali, F. Campagna, and N. Kalaany for assistance in obtaining human blood samples; M. Brown, J. Goldstein, and D. W. Russell for helpful discussions; J. Kastelein and J. C. Defesche for providing genomic DNA from an Iranian ARH patient; and A. K. Khachadurian, M. J. Chapman, J. L. DeGennes, and J. M. Hoeg for providing skin fibroblasts from ARH patients and M. Brown and J. Goldstein for making them available to us. Supported by POI-HL2048, the W. M. Keck Foundation and the Donald W. Reynolds Cardiovascular Clinical Research Center (H.H.H.), Telethon grant E. 0565 (M.A.), and NIH training grant HL07360 (K.W).

6 March 2001; accepted 9 April 2001
Published online 26 April 2001;
10.1126/science.1060458
Include this information when citing this paper.